ACS EARTH AND SPACE CHEMISTRY

http://pubs.acs.org/journal/aesccq

Article

Aerosol Mass Spectral Profiles from NAMaSTE Field-Sampled South Asian Combustion Sources

J. Douglas Goetz,* Michael R. Giordano, Chelsea E. Stockwell, Prakash V. Bhave, Praveen S. Puppala, Arnico K. Panday, Thilina Jayarathne, Elizabeth A. Stone, Robert J. Yokelson, and Peter F. DeCarlo*

Cite This: *ACS Earth Space Chem.* 2022, 6, 2619−2631

Read Online

ACCESS | Metrics & More | Article Recommendations | Supporting Information

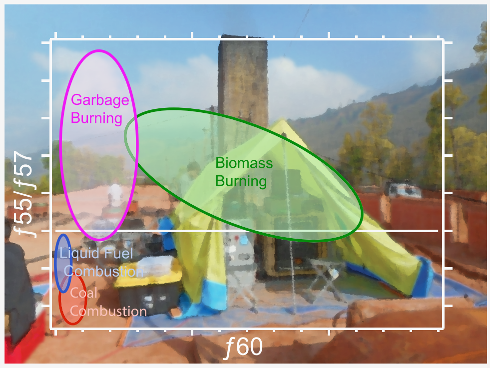

ABSTRACT: Unit mass resolution mass spectral profiles of nonrefractory submicron aerosol were retrieved from undersampled atmospheric emission sources common to South Asia using a "mini" aerosol mass spectrometer. Emission sources including wood- and dung-fueled cookstoves, agricultural residue burning, garbage burning, engine exhaust, and coal-fired brick kilns were sampled during the 2015 Nepal Ambient Monitoring and Source Testing Experiment (NAMaSTE) campaign. High-resolution peak fitting estimates of the mass spectra were used to characterize ions found within each source profile and help identify mass spectral signatures unique to aerosol emissions from the investigated source types. The first aerosol mass spectral profiles of dung burning, charcoal burning, garbage burning, and brick kilns are provided in this work. The online aerosol mass spectra show that organics were generally the dominant component of the nonrefractory aerosol. However, inorganic aerosol components including ammonium and chloride were significant in dung- and charcoal-fired cookstove emissions and sulfate compounds were major components of the coal-fired brick kiln emissions. Organic mass spectra from both the charcoal burning and zigzag brick kiln were dominated by nitrogen-containing ions thought to be from the electron ionization of amines and amides contained in the emissions. The mixed garbage burning emissions profiles were dominated by plastic combustion with very low fractions of organic markers associated with biomass burning. The plastic burning emissions were associated with enhanced organic signal at mass-to-charge (m/z) 104 and m/z 166, which could be useful fragment ion indicators for garbage burning in ambient aerosol profiles. Finally, a framework for the identification of emission sources using the unit mass resolution organic mass fractions at m/z 55 (f_{55}), m/z 57 (f_{57}), and m/z 60 (f_{60}) is proposed in this work. Plotting the ratio of f_{55} to f_{57} versus f_{60} is found to be effective for the identification of emissions by the fuel type and even useful in separating emissions of similar source types. Although the sample size was limited, these results give further context to the aerosol and gas-phase emission factors presented in other NAMaSTE works and provide a critical reference for future aerosol composition measurements in South Asia.

KEYWORDS: *South Asia, aerosol emissions, aerosol mass spectrometry, brick kiln, garbage burning, biomass burning*

1. INTRODUCTION

Aerosol emissions from prevalent but poorly understood combustion sources in South Asia impact public health,[1] influence local and regional air quality,[2−5] and have uncertain direct and indirect climate forcing impacts.[6] Additionally, aerosol pollutants from South Asia are effectively transported into the lower stratosphere via the Asian Summer Monsoon anticyclone mechanism.[7] Solid fuels in the form of biomass or coal are commonly used throughout South Asia in the industrial sector[8−10] and are predominant for residential cooking and heating in the region.[11,12] Because solid fuel combustion is a strong emitter of gaseous and particle phase pollution, residential solid fuel use has been ranked the primary risk factor for disease in South Asia[13] and it is a major source of emissions for the region.[14] In addition to solid fuel combustion, the combustion of petroleum-based fuels by light and heavy-duty vehicles is a major source of aerosol and gas-phase pollution in Asia that has been rapidly increasing.[15−17] Because both the chemical characteristics and amount of primary aerosol emissions from solid biofuel and fossil fuel combustion in South Asia are poorly understood, there is uncertainty in the relative contribution of the two emission sources, which has led to differences in emission inventories as well as contradictory results from top-down and bottom-up regional emission estimates.[6,18] The uncertainties in the aerosol emission inventories of South Asia indicate that there is a need for improved source apportionment in the region.

Received: June 8, 2022
Revised: September 28, 2022
Accepted: October 6, 2022
Published: November 3, 2022

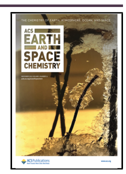

Additionally, the limited source apportionment studies that have been conducted reveal that variability in the chemical profiles of aerosol emissions and volatile organic compounds from South Asian combustion sources have led to additional uncertainties in apportionment models.[19−26]

To expand the current understanding of atmospheric pollution in South Asia, field research was conducted as part of the Nepal Ambient Monitoring and Source Testing Experiment (NAMaSTE) in Nepal in 2015. NAMaSTE had two major components: (1) ambient monitoring in the Kathmandu Valley to investigate ambient air quality and for source apportionment modeling and (2) to characterize aerosol and gas-phase emissions from important and under-characterized emission sources in South Asia. Sources included brick-making kilns, agricultural residue burning, traditional and improved cookstoves operated with a variety of fuels, open garbage burning, diesel-powered ground water pumps used for crop irrigation, and idling motorcycles. Detailed descriptions of the investigated emission sources can be found in Stockwell et al.[27] Here, we used on-line aerosol measurements to characterize the chemical composition of submicron aerosol (PM_1) from the investigated emission sources and to evaluate marker ions. Aerosol mass spectrometry was used to characterize the mass spectra of nonrefractory PM_1 and is completed in tandem with Part 1 of the study, which quantified speciated PM_1 emission factors using on-line aerosol and gas-phase instrumentation.[28] Other NAMaSTE papers involved with the source testing aspect of the campaign include Stockwell et al., who reported gas-phase emission factors and aerosol optical properties, and Jayarathne et al.,[27] who reported off-line filter-based emission factors of fine aerosol ($PM_{2.5}$), organic carbon, elemental carbon, inorganic ions, organic molecular markers, trace metals, and PAHs. This work links the NAMaSTE source testing with ambient source apportionment work by Werden et al.[30] that took place in the Kathmandu Valley in Nepal in 2015 and more recently. The AMS mass spectral profiles reported in this work are the first available for major undersampled sources in South Asia and important as such, but additional measurements could improve the representativeness or specificity available in the future.

2. METHODOLOGY

2.1. Source Sampling. The NAMaSTE source sampling took place in April 2015 in several regions of Nepal including the Kathmandu Valley, Central Nepal, and the Tarai region that is part of the Indo-Gangetic Plain bordering India. Engine exhaust sources included two diesel-powered ground water pumps that are used for crop irrigation and four idling four-stroke motorcycles sampled directly after servicing. We sampled two brick kilns, which included a traditional batch-style clamp kiln and a more advanced continuous firing forced draft zigzag kiln.[31] Both kilns were fueled with coal, but the clamp kiln was also cofired with hardwood, and bagasse was used as a starter fuel at the zigzag kiln. Several types of open garbage burning were sampled including two mixed refuse piles, segregated plastics, which were primarily composed of plastic films, and segregated metalized plastic or foil "chip bags". The refuse mixes were composed of unmeasured quantities of paper, cardboard, plastics, food waste, yard waste, and other common household garbage. Biomass burning sources included crop residue burning and cooking stoves. The agricultural residue included a mix of wheat straw, lentils, mustard, and grasses. Other segregated burns included wheat straw, mustard, and locally sourced grasses. Cooking stoves were sampled in the field at residences in the Tarai region and in a lab setting at the Nepal Renewable Energy Test Station (RETS). The field-tested samples included two single-pot traditional mudstoves fueled with either hardwood sticks (mostly Baikano) and twigs (mostly *Shorea robusta*), or dung logs, and one two-pot traditional mudstove cofired with hardwood and dung logs. None of the field-tested stoves had a chimney, and all tests, but the single-pot dung burning test, were conducted during either the morning or evening cook cycles. The cooking typically consisted of rice, lentils, and curry. Meat cooking or deep frying was not sampled during these tests, which suggests that the food cooking likely had a little impact on the organic aerosol emissions compared to the fuel. It should be noted that an attempt was made to sample well-mixed emissions from the field-tested cookstoves similar to what a resident would typically be exposed to during a cook cycle. The lab-tested traditional cookstoves included a single-pot mudstove and a three-stone cooking fire. Each traditional stove was fueled with fuelwood, dung, or a mix of the two. The lab-tested improved cookstoves included a mudstove with a chimney fueled with hardwood and dung, an Envirotech natural draught stove fueled with hardwood and dung, a forced draft stove fueled with hardwood, a bio-briquette charcoal stove, a Bhuse Chulo fueled with sawdust and hardwood, and a biogas stove (see Table S2 of Jayarathne et al. for photographs and additional descriptions of these stoves). Details on sampling durations and sampling methods at each emission source can be found in Part 1 of this study,[28] whereas details on the operation and fuels of each source can be found in Stockwell et al. It should be noted that no unexpected or unusually high safety hazards were encountered while sampling the above listed emission sources. On average, 123 aerosol mass spectra of emissions samples were collected per source. This provided about 20 min of emissions data per source, which varied depending on inlet location with respect to the wind direction, equipment and instrument performance, duration of the background and filter sampling periods, and burn or run time of each experiment. The on-line sampling was conducted with a dilution system to simulate ambient state particle-to-gas partitioning of semivolatile organic compounds contained in a cooled and dilute emission plume. The diluted flow system was comprised of a Dekati Ltd. axial diluter (DAD-100) that provided ~16 SLPM HEPA filtered air to the sample flow. Dilution factors ranged from ~20:1 to 1:1 with an average of 10:1 and were chosen based on plume proximity and source strength. Average dilute organic aerosol mass concentrations ranged from about 20 to 160 $\mu g/m^3$ with an average of 80 $\mu g/m^3$ for the entire study. More on the dilution and sampling system used during NAMaSTE can be found in the methods section of Goetz et al.[28] A table of the investigated emission sources and corresponding fuel type can be found in Table S1 of the Supporting Information.

2.2. Instrumentation. Aerosol mass spectral profiles were retrieved using an Aerodyne Inc. "mini" aerosol mass spectrometer (mAMS). The mAMS is functionally similar to a compact time-of-flight aerosol mass spectrometer (c-TOF-AMS),[32] but with a smaller vacuum chamber and time-of-flight mass spectrometer. Additionally, the body, the split-cell turbo vacuum pump, and electronics are similar to an Aerodyne Inc. time-of-flight aerosol chemical speciation monitor (TOF-ACSM),[33] but the mAMS contains a chopper system for particle time-of-flight sizing and aerosol signal control in

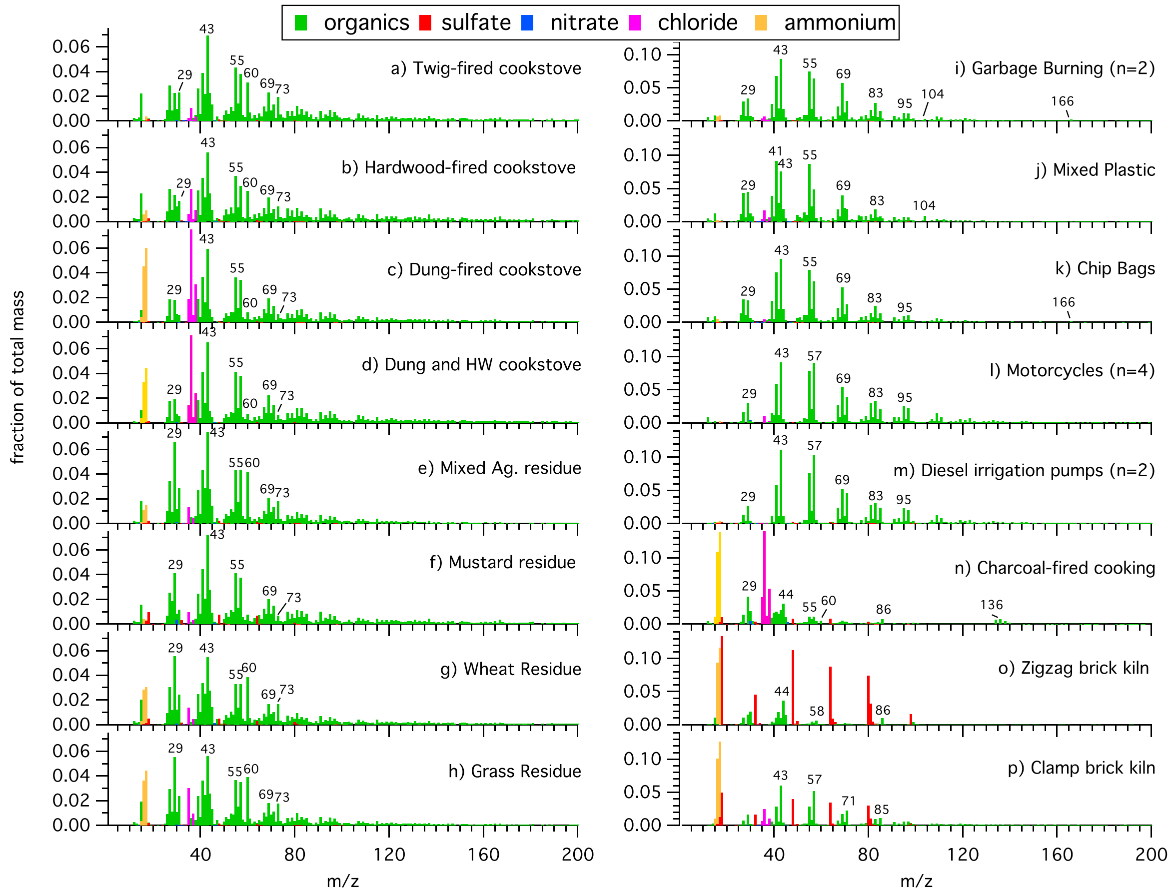

Figure 1. Average mass spectra of nonrefractory submicron aerosol emissions as a function of average total mass from the field-tested emission sources measured with the mAMS. Sample number is 1 unless otherwise indicated.

addition to a more advanced data acquisition card. The mAMS was operated in mass spectrum mode, and all mass spectra were averaged to an effective sampling rate of 0.1 Hz. All mass spectra were collected at a mass-to-charge (m/z) range of 10–295 (upper limit for instrument) at unit mass resolution (UMR). The standard tungsten vaporizer was operated at 600 °C. All data processing and analysis was done in Igor Pro 6.3 (Wavemetrics, Lake Oswego, OR) using standard TOF-AMS analysis software SQUIRREL v1.57I and PIKA v1.16I. Although data from the mAMS is generally presented in unit mass resolution (UMR), the data was processed using high-resolution peak fitting in the PIKA module. The module was used to reduce errors related to large and dynamic aerosol loadings that cannot be efficiently resolved using the static fragmentation table associated with SQUIRREL and employed to separate aerosol mass spectral signal from gas-phase signal (i.e., CO_2, O_2, N_2, etc.).[34] High-resolution treatment of moderate resolution mass spectral data has previously been performed by other researchers using the TOF-ACSM.[33] Coincident carbon dioxide (CO_2) measurements using a Picarro Inc. cavity ring down spectrometer (CRDS) were used for time-dependent subtraction of gas-phase loading at m/z 44 as described in Collier and Zhang[35] and is standard postprocessing for Aerodyne mass spectrometer sampling within dynamic CO_2 environments. The gas-phase CO_2 and aerosol-only m/z 44 difference mass spectral signal were typically within a factor of 2 in NAMaSTE because of the aerodynamic lens, chopper, and differential pumping system, which effectively removes most of the air signal. Details on the Picarro Inc. CRDS operation and CO_2 calibration can be found in Goetz et al. (section 2.2.4).[28]

3. RESULTS AND DISCUSSION

3.1. Mass Spectral Signatures. The average UMR mass spectral profiles of organics, sulfate, nitrate, chloride, and ammonium of the field-tested emissions can be found in Figure 1 as fractions of total nonrefractory submicron aerosol (NR-PM_1) mass. The mass spectral profile for a charcoal-fueled cookstove sampled at RETS is included in Figure 1 because charcoal burning was not sampled in the field and it provides unique results. Generally, organic aerosol comprised the largest fraction of the nonrefractory emissions with the exception of sulfate at the coal-fired zigzag kiln (Figure 1p). The organic only average mass spectra normalized to total organic mass and 1σ variability from each field-tested emission source can be found in the Supporting Information. Inorganic chloride and ammonium were found to make up a large fraction of NR-PM_1 emissions from the traditional biomass burning sources (e.g., crop residue burning and biomass-fueled cookstoves) and the clamp kiln. Open garbage burning was also observed to have a significant fraction of chloride, and the engine exhaust sources were observed to have negligible fractions of inorganic aerosol. It should be noted that inorganic nitrate aerosol mass fractions were low in all of the sampled emission sources with an average of 0.22 ± 0.24% of the total nonrefractory aerosol observed by the mAMS. This is in agreement with the low inorganic nitrate aerosol mass observed with filter sampling by Jayarathne et al.[29] A discussion of the mass spectral profiles for each source type can be found below.

3.1.1. Wood-Fueled Cookstoves. The average organic aerosol fragmentation for the field-tested wood-fueled cookstoves (Figure 1a,b and Figure S1) followed what has previously been observed with wood burning[36−38] containing organic mass spectral peaks at m/z 29 ($C_2H_5^+$ and CHO^+), m/z 55 ($C_4H_7^+$ and $C_3H_3O^+$), m/z 57 ($C_4H_9^+$ and $C_3H_5O^+$), m/z 60 ($C_2H_4O_2^+$), m/z 69 ($C_5H_9^+$ and $C_4H_5O^+$), m/z 73 ($C_3H_5O_2^+$), m/z 91 (benzyl ion, $C_7H_7^+$), m/z 115 ($C_9H_7^+$ and $C_8H_3O^+$) and m/z 137 (likely $C_8H_7O_2^+$). Levoglucosan, a by-product from the pyrolysis of cellulose, has been shown to produce the organic ion fragments at m/z 29, 60, and 73 and is a well-documented marker for biomass burning.[36,39,40] The ion fragments at m/z 55 and 69 make up part of the UMR ion series $C_nH_{2n-1}^+$ and $C_mH_{2m-1}CO^+$, and m/z 29 and 57 make up part of the ion series $C_nH_{2n+1}^+$ and $C_mH_{2m+1}CO^+$. These ion series are typically produced from electron ionization (EI) of saturated hydrocarbon compounds including alkanes, alkenes, and cycloalkanes.[41] Ions found at m/z 91, m/z 115, and m/z 137 are thought to be produced from the combustion of lignin, a fibrous compound that is found in plants, and have previously been observed with an aerosolized lignin powder mass spectrum retrieved from the AMS mass spectral database.[42,43]

Average organic mass spectra for the individual wood-burning only cookstove experiments in NAMaSTE, RETS lab sampling included, can be found in Figure S2 of the Supporting Information. The organic profiles from the two field-tested single-pot mudstoves indicate that there was excellent correlation in the relative organic fractions between the stick and twig-fueled emissions and the hardwood log-fueled emissions (Pearson's r = 0.99). Although well correlated, a slightly larger organic fraction was found at m/z values above 200 from stick burning compared to hardwood burning (3.6% greater), which has previously been associated with signal from high-molecular-weight polycyclic aromatic hydrocarbons (PAH).[44] A list of PAHs observed from the NAMaSTE sampled cookstove emissions and their fuel-based emission factors can be found in Jayarathne et al.[29]

Comparisons of the hardwood-fueled traditional and improved cookstoves at RETS to the field-tested hardwood-fueled stove indicate that there is good correlation between the tests with Pearson's r values ranging from 0.87 to 0.93 (Figure S2). Additionally, the regressions with slopes >1.16 indicate that some differences existed between the emission sources. One major difference between the field and lab mass spectra was the enhanced organic m/z 29 fraction observed with the lab-tested stoves. The field-tested stove produced an average f_{29} (fraction of organic signal at m/z 29 to total organic mass) of 0.023, and m/z 43 was the dominant organic peak in the mass spectrum. The lab-test stove emissions, however, were observed to have the largest organic peak at m/z 29, and the average f_{29} ranged from 0.067 to 0.087 for the improved cookstoves and was 0.082 for the three-stone traditional stove. In addition to differences in individual organic peaks, the lab-tested cookstoves were observed to have a reduced fraction of organics at m/z values greater than 100. The percentage of organic mass above m/z 100 ranged from 13 to 18% with the lowest percentages observed from the three-stone fire and the forced-draft improved stove compared to the >22% observed from the field-tested stoves. The lab-tested stoves were observed to have more efficient burn conditions with average modified combustion efficiency (MCE) values ranging from 0.955 to 0.984.[27] Therefore, the lower fraction of high-molecular-weight ion fragments combined with the larger f_{29} values observed from the lab-tested stoves suggests more easily fragmented organic functional groups were contained in the lab-tested aerosol emissions compared to the field-tested stove, which was likely due to the increased efficiency of the lab-tested stoves. Similar results were observed in a comparison between the organic profiles of the field-tested stoves and lab tests of Puerto Rican hardwood burning and average observations of biomass burning organic aerosol[37] (Figure S2), both of which were retrieved from the AMS mass spectral database.[42,43] Additionally, the hardwood-fired lab-tested stoves were observed to have a ∼30% greater elemental carbon-to-organic carbon ratio compared to the field-tested stoves.[29] This reveals that the field-tested stoves likely had more smoldering phase emission that produced unique mass spectral characteristics compared to lab-based wood burning. The larger emissions of low burn efficiency-related organic functional groups by traditional mudstoves, and possibly increased emissions of PAHs, should therefore be considered in indoor exposure modeling and in source apportionment studies.

3.1.2. Dung-Fueled Cookstoves. The dung burning emissions observed in NAMaSTE are characterized as containing large fractions of inorganic ammonium and chloride (Figure 1c,d, Figure S3). The chloride content ranged from 9 to 23% of the total NR-PM_1 mass with an average of 15%. The ammonium ion content ranged from 7 to 20% of total NR-PM_1 mass with an average of 12%. Similar inorganic aerosol mass fractions were observed from these emission sources by the NAMaSTE offline filter-based sampling.[29] In comparison, the field-tested hardwood-fueled stove emissions were observed to contain 1.5% ammonium and 4.3% chloride, and lower fractions were observed from the RETS hardwood-fueled stoves. The observed inorganic fraction from the dung-fueled and dung-cofired stoves appeared to be independent of the sampling location, stove type, and dung content of the fuel. In addition to containing large fractions of chloride, the chloride itself was composed of >80% HCl^+ ion (m/z 36 and the isotope at m/z 38) indicating the possibility of the some amount of phase partitioning of gaseous HCl emissions. Size distribution data presented in the companion paper reveals that the chloride aerosol was found at similar sizes to the ammonium aerosol indicating that the components were likely internally mixed and the chloride was neutralized to some extent by the ammonium cations.[28]

The organic aerosol profiles from dung-fueled emissions were found to have similar patterns to wood burning emissions but with some key differences. Based on the six dung burning samples, two with pure dung and four cofired with hardwood, from both the field and lab, organic aerosol mass spectra had major peaks associated with the ion series $C_nH_{2n-1}^+$, $C_mH_{2m-1}CO^+$, $C_nH_{2n+1}^+$, and $C_mH_{2m+1}CO^+$ (Figure S3). The dung burning samples also had notable peaks from ions at m/z 60, m/z 73, m/z 91, and m/z 115, which had previously been observed with the wood burning, and an isolated peak at m/z 165. Generally, the organic profiles had similar patterns and all of the samples were well correlated to the field-tested dung-fueled cookstove with Pearson's r values ranging from 0.95 to 0.98 (Figure S3). The best correlation was observed between organic emission from the two field-tested samples indicating that dung was the primary emitter from the two-pot stove and wood burning had little influence on the cofired organic profile. Additionally, the levoglucosan markers emitted from the pure and cofired dung burning (*m/z* 60 and 73) were observed to comprise a smaller fraction of the total organic mass compared to hardwood burning. For example, f_{60} from the dung burning samples had an average of 0.012, compared to an f_{60} of 0.026 from the hardwood-fueled stove emissions observed in the field. f_{73} was observed at an average of 0.009 from dung burning compared to the field-tested hardwood burning, which had an f_{73} of 0.13. Since the levoglucosan ions are used as markers for traditional biomass burning and to understand the photochemical aging of biomass burning aerosol,[45] the low fractions observed from pure and cofired dung burning could complicate ambient observations when dung burning is part of a source profile. It should be noted that, aside from the low fraction of biomass burning markers, there are few other distinctions between organic aerosol of the field-tested wood burning samples and the pure dung burning samples (Pearson's r = 0.95). The similarities between the organic mass spectra of wood burning and dung burning suggest that differences in inorganic mass fractions (i.e., ammonium and chloride) or other measurement techniques like off-line gas chromatograph mass spectrometry (GC−MS) may be needed to distinguish dung burning emissions from wood burning emissions in ambient datasets collected with UMR AMS. For example, trace organic compounds including fecal sterols and stanols have been identified as molecular markers from filter-based off-line GC−MS analysis of dung burning emissions.[29,46]

3.1.3. Improved Cookstoves with Other Fuel. Emissions from other improved cookstoves including a biogas stove and a biobriquette stove were sampled at RETS. The biogas stove was fueled with locally produced cow dung biogas (likely primarily composed of methane), and it is important to note that NR-PM$_1$ mass was not observed to increase above the background level while the biogas stove was operational. Therefore, we cannot comment on the mass spectral profile from biogas burning, but we can confirm it is a "cleaner" fuel similar to LPG. The biobriquette stove was fueled with charcoal briquettes.

The NR-PM$_1$ emissions from the charcoal biobriquette stove produced unique mass spectra compared to the other NAMaSTE tested cookstoves, and to our knowledge, this work is the first to characterize the mass spectral profile of biobriquette charcoal combustion emissions. Generally, the charcoal emissions were observed to have high inorganic fractions and the average nonrefractory mass was comprised of 42.3% organic, 27.5% chloride, 25.9% ammonium, 3.9% sulfate, and 0.3% nitrate (Figure 1n). The observed chloride and ammonium fractions were the largest of any of the combustion sources investigated in this work. In addition to containing a unique inorganic fraction, the average organic spectrum was observed to have distinct mass spectral signals. Major organic peaks included ion fragments common with biomass burning (*m/z* 29, 57, 60, etc.), but also included characteristics peaks at *m/z* 44, *m/z* 64, *m/z* 86, and a grouping of peaks centered at *m/z* 136 (Figure 1n). Many of these organic peaks, and others not listed but observed with charcoal emissions, were not observed to the same extent from hardwood burning. Additionally, some organic ions found at *m/z* values greater than 200, which have been associated with PAHs,[44] were observed at a higher fraction from charcoal burning than wood burning. Based on the high-resolution peak fitting estimates of the raw mass spectral data, the organic ions at *m/z* 44, *m/z* 64, and *m/z* 86 correspond to nitrogen-containing organics $C_2H_6N^+$, $C_4H_2N^+$, and $C_5H_{12}N^+$, respectively. An example of the peak fitting estimates at *m/z* 44 can be found in Figure 2. The figure shows that CO_2^+, $C_2H_4O^+$,

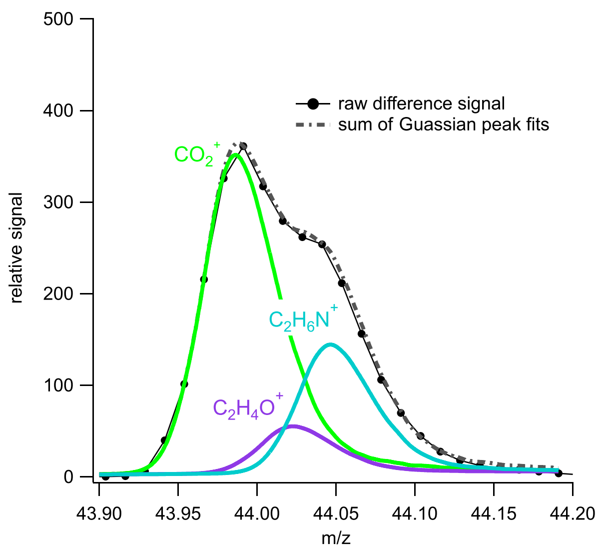

Figure 2. High-resolution peak fitting of average raw mass spectral signal at *m/z* 44 for charcoal combustion from a biobriquette stove.

and $C_2H_6N^+$ produce a good fit to the raw UMR difference signal at *m/z* 44, which indicates that $C_2H_5N^+$ is likely a major component of the organic signal at that position. Similar results were observed at *m/z* 64 and *m/z* 86, and the listed ions have previously been attributed to nitrogen-containing organic compounds in ambient datasets.[47,48] Additionally, electron ionization of aliphatic primary amides has been observed to generate peaks at *m/z* 44 and *m/z* 86.[49] We could not positively identify nitrogen-containing organic ions at *m/z* 136 because of the larger peak width and more numerous potential ions compared to the lower *m/z* peaks, and the peak has not been observed with nitrogen-containing organics spectra in the literature. The grouping of organic ions centered at *m/z* 136 remains unidentified, but they are possibly due to chloride-containing organic fragment ions with the formula $C_2H_5Cl_3$ based on an isotopic pattern (see the Supporting Information, Figure S8). More sampling of charcoal emissions is needed to understand if the mass spectral characteristics of biobriquette charcoal combustion observed in this study are ubiquitous with other types of charcoals and under different burn conditions.

3.1.4. Agricultural Residue Burning. The average NR-PM$_1$ mass spectra for the agricultural residue burning samples can be found in Figure 1e−h and Figure S4. The crop residue samples were observed to have mass spectra similar to the wood burning samples with moderate fractions of inorganic compounds and organic fragmentation that features peaks associated with cellulose and lignin combustion. The largest inorganic mass fraction was observed from grass burning, and the emissions were likely well neutralized with an average ammonium fraction of 0.08, an average chloride fraction of 0.04, and nominal fractions of sulfate and nitrate. Neutralized inorganic aerosol was also observed from the mixed crop residue and wheat residue burns. Mixed residue NR-PM$_1$ emissions were composed of 2.7% ammonium and 1.7% chloride. Wheat residue emissions were composed of 6.0%

https://doi.org/10.1021/acsearthspacechem.2c00173
ACS Earth Space Chem. 2022, 6, 2619−2631

ammonium and 1.7% chloride. Mustard residue emissions were less neutralized and were observed to have inorganic fractions <0.01. The organic aerosol emissions from the crop residue burning samples were observed to have relatively similar mass spectral patterns. Comparisons of organic spectra from the segregated residue burns to the mixed residue burn reveal that the Pearson's r correlation between the samples are >0.9 with 0.94 for mustard residue, 0.99 for wheat residue, and 1.00 for grass residue. The lower correlation associated with the mustard residue and mixed residue was due to the lower fraction of organic ions associated with levoglucosan and the 10% greater fraction of organic ions found at m/z peaks above 100.

3.1.5. Open Garbage Burning. The open garbage burning samples were characterized as having low inorganic aerosol fractions and organic aerosol with major mass spectral patterns that follow the saturated hydrocarbon ion series (Figure 1i–k). The mixed garbage samples were visually observed to contain biomass materials like paper and yard waste, but the mixes were found to produce small fractions of levoglucosan and lignin organic ion fragments that have been discussed with the biomass burning samples. Based on high-resolution peak fitting, the mass spectral data of the garbage burning samples had larger fractions of $C_nH_{2n+1}^+$ and $C_nH_{2n-1}^+$ ions compared to their oxygenated ion series counter parts, which were observed at almost equal fractions to the alkyl ions in the biomass burning samples. Consequently, other materials contained in the mixes (e.g., plastics) likely had a large influence on the organic aerosol composition from open garbage burning. The two garbage mixes were found to have differences in aerosol emission factors, which were thought to be due to differences in fuel composition and water content.[28,29] Nonetheless, the organic mass spectra for the two mixes were well correlated (Pearson's r = 0.95). The two segregated plastic burns, which included metalized plastic "chip bags" and mixed plastics, were found to have organic mass spectra that were well correlated to the combined mixed garbage samples. The Pearson's r value between the garbage mix and metalized plastic was 0.99, and the mix was found to be slightly less correlated to the plastic burn with a value of 0.96. The strong correlation between the plastic emissions and mixed garbage combined with the low fractions of organic ions related to biomass burning indicates that plastic burning aerosol dominated the mass spectral emission profile from the sampled garbage mixes. These are the first field-measured AMS mass spectral profiles of open garbage burning, and they provide a valuable start for studies of aerosol in South Asia and other parts of the world where refuse burning is prevalent.[46]

Two notable, relatively high-molecular weight organic ions were observed with the open garbage burning samples that were not seen with other tested emission sources, and each was attributed to burning of different types of plastics. A prominent ion signal at m/z 104 was observed with the mixed plastic burning emissions (Figure 1j). An organic peak at m/z 166 was observed with metalized plastic burning (Figure 1k). Because both peaks are greater than 100 amu and have large peak widths, with many potential ion contributions, high-resolution fitting estimates based on the UMR data could not be used to obtain more information about these organic ions. However, inferences can be made based on existing literature. The large fraction of m/z 104 associated with mixed plastic burning is thought to be due to the styrene ion ($C_8H_8^+$) based on comparisons to NIST EI mass spectra.[51] The styrene ions are fragments from larger molecular species likely from aerosols produced from the combustion of polystyrene, acrylonitrile-butadiene-styrene (ABS),[40] or similar plastics as observed with plastic no. 6, burning by Mohr et al.[41] As expected, styrene ions were not observed from metalized chip bag burning as that plastic is typically composed of layers of low-density polyethylene (LDPE), aluminum, and vapor barrier polymers that do not contain styrene compounds.[52] The origin of organic ion peak at m/z 166 observed with chip bag combustion is uncertain but is possibly from an ion fragment consistent with the structure of fluorene.[51] These unique garbage burning ions could be good candidates as UMR and high-resolution indicators of open garbage burning in South Asia and complimentary garbage burning aerosol tracers, which prior to this work included 1,3,5-triphenylbenzene (TPB),[29,53] elemental antimony (Sb),[40] and phthalates.[54,55]

3.1.6. Engine Exhaust. Two ground water irrigation pumps and four idling motorcycles were the only liquid-fuel emission sources sampled by the mAMS during NAMaSTE. Organic aerosol was the dominant fraction of the NR-PM_1 emissions of both source types, and most inorganic aerosol components were below detection limits (Figure 1). The irrigation pumps were ∼5kVA diesel powered and had different operational lifetimes. One pump was a Kirloskar (model unknown) that was in operation for ∼3 years (Pump 1), and the other was a Field Marshall model R170a (Pump 2) that had been recently purchased. Although the newer pump was observed to have a lower organic aerosol emission factor compared to the older pump,[28] the bulk organic mass spectra of the emissions were very well correlated (Pearson's r = >0.99). The average mass spectra from the two pumps had major ion peaks associated with the saturated hydrocarbon series $C_nH_{2n+1}^+$ and $C_nH_{2n-1}^+$, and the largest organic fractions were at m/z 41 (C_3H_5+), m/z 43 ($C_3H_7^+$), m/z 55 ($C_5H_7^+$), and m/z 57 ($C_4H_9^+$) with the dominant ions being $C_3H_7^+$ and $C_4H_9^+$ (Figure 1m). These major ion peaks coincide with previous UMR measurements of diesel vehicle emissions and engine lubricating oil.[41,56] Additionally, the organic mass spectra from the combined pump emissions were also well correlated to the average HOA spectrum of Ng et al.[54] with a Pearson's r of 0.97.

The four gasoline-powered idling 4-stroke motorcycles did not produce inorganic fractions above detection limits, and based on the average organic mass spectra, the emissions produced spectral patterns almost identical to the diesel sources (Figure 1l). The average organic mass spectrum was dominated by ions associated with the ion series $C_nH_{2n+1}^+$ and $C_nH_{2n-1}^+$. Based on estimated high-resolution peak fitting, $C_4H_9^+$ found at m/z 57 was the most abundant organic ion. The time-resolved data indicates f57 had a narrower mass fraction range compared to the irrigation pumps with a 10th percentile of 0.088 and a 90th percentile of 0.10, with a median at 0.099. Overall, the average organic mass spectrum from the motorcycle emissions was well correlated to the average diesel irrigation pump profile with a Pearson's r of 0.98. Furthermore, the average idling motorcycle profile was found to have a similar percentage of ions above m/z 100 (∼15%) compared to the irrigation pump profile. The results indicate that, from the observed compositional perspective, the liquid-fueled engines investigated in NAMaSTE produced similar organic aerosol.

3.1.7. Brick Kilns. Emissions from a low efficiency batch-style clamp brick kiln that was fired with coal and hardwood were sampled in NAMaSTE. The average mass spectral profile

https://doi.org/10.1021/acsearthspacechem.2c00173
ACS Earth Space Chem. 2022, 6, 2619−2631

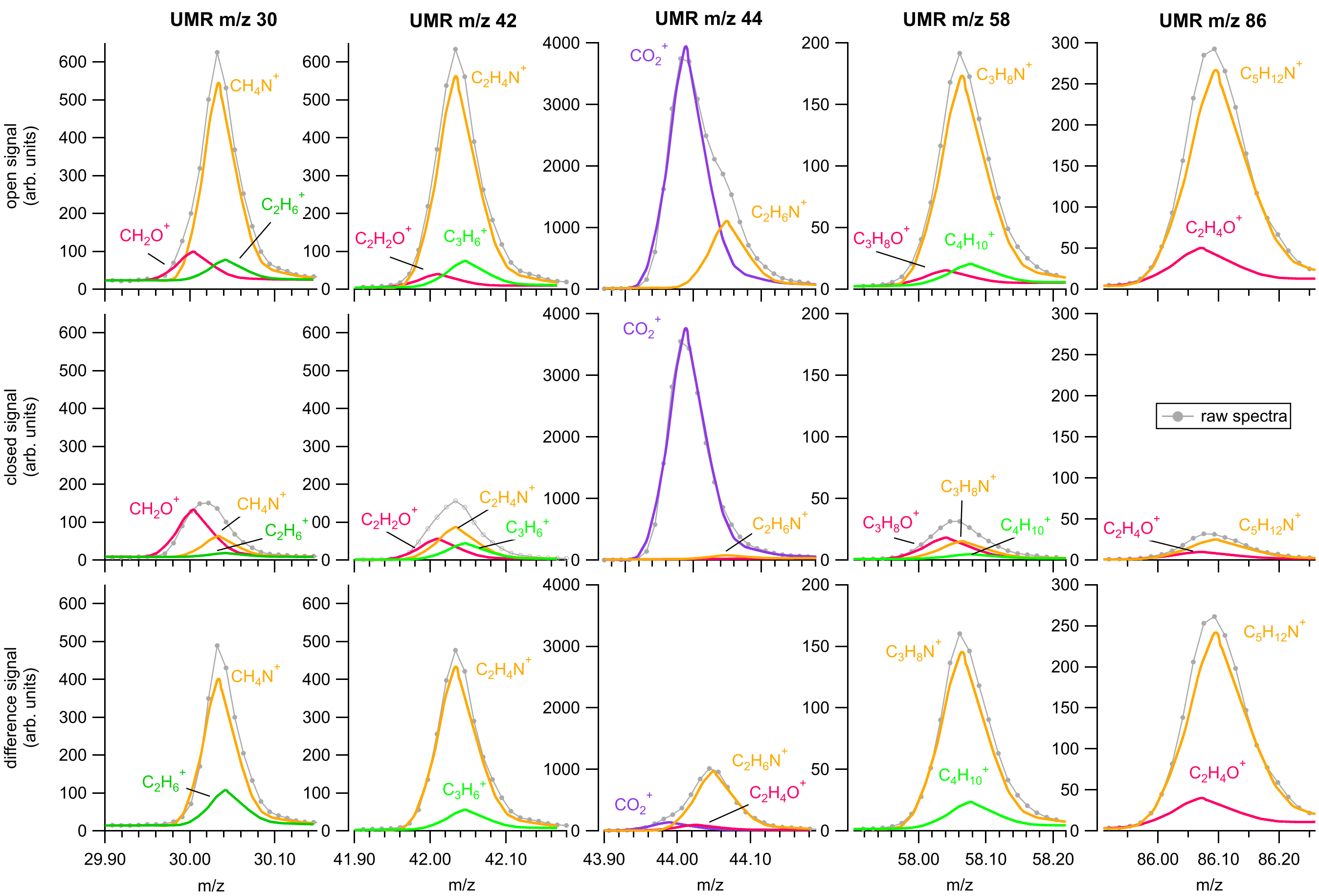

Figure 3. Average open, closed, and difference high-resolution peak fitting estimates of major UMR peaks associated with zigzag brick kiln emissions.

from the kiln emissions shows that inorganic aerosol was a major component of the total NR-PM$_1$ mass at approximately 50% (Figure 1p). Ammonium and sulfate were the primary inorganic components at ~24.0 and 21.0% of the total mass, respectively, followed by chloride (4.3%), and nitrate (<1%) (Figure 1p). Similar results in the aerosol fraction were observed in the NAMaSTE filter-based measurements, but with sulfate mass ~30% greater than ammonium based on the average emission factors.[29] Based on the large ammonium fraction reported by the mAMS, the ammonium mass is in excess of what is needed for full neutralization of sulfate, chloride, and nitrate indicating likely other anions are present (e.g., organic acids) and neutralized by ammonium. The average organic aerosol profile contained patterns that were similar to HOA and engine exhaust with large fractions observed with the $C_nH_{2n-1}^+$ and $C_nH_{2n+1}^+$ ion series from alkyl fragments. The similarity to HOA may be due to the use of used motor oil, which can be added to brick kiln fuel as a coloring agent, and was discussed in Stockwell et al. as a possible source of the abundant gas-phase alkanes observed in the clamp kiln emissions. Based on peak fitting estimates, very low fractions of the $C_nH_{2n+1}CO^+$ and $C_nH_{2n-1}CO^+$ were observed. The average f_{43} was 0.12, and the average f_{57} was 0.10. Also, like engine exhaust emissions, significant fractions of $C_nH_{2n-3}^+$ ions were observed and specifically m/z 67, 71, and 81 (Figure 1q). Large fractions of $C_nH_{2n-3}^+$ have previously been attributed to EI of cycloalkanes.[49] Unlike engine exhaust, however, the alkyl fragment series at C$_5$ and C$_6$ within the $C_nH_{2n+1}^+$ ions were observed to comprise a larger fraction of the organic mass compared to their $C_nH_{2n-1}^+$ counterpart (Figure 1n). Similar alkyl fragmentation has previously been observed with aerosolized diesel fuel[56] and further suggests the use of motor oil in the kiln fuel. The low fractions of oxygenated ions at m/z 43, m/z 55, and other ions in the saturated hydrocarbon ion series suggests that the wood fuel emissions were limited compared to coal since oxygenated ions in the series are common with the NAMaSTE sampled wood-burning emissions and with BBOA.[37] Further evidence for the low fraction and/or relatively efficient combustion of wood fuel is demonstrated by the low fraction of levoglucosan ions (average f_{60} = 0.0007) observed in the clamp kiln emissions. There have been limited measurements of coal burning aerosol with AMS instrumentation, and to our knowledge, this work is the first to characterize direct emissions. One study that deconvolved ambient measurements in China to produce PMF spectra for coal combustion found characteristic organic peaks at m/z 128 (ion fragment corresponding to naphthalene), m/z 152 ($C_7H_6NO_3^+$ and $C_9H_{12}O_2^+$), and m/z 178 ($C_{14}H_{10}$).[57] Based on the average organic mass spectrum from the clamp kiln emissions, f_{128} was 0.0035, f_{152} was 0.0026, and f_{178} was 0.002, and none of the listed m/z stood out as prominent peaks. The results indicate that factors like the coal type and quality in addition to plume aging may influence the relative contribution of the tracer ions observed by Hu et al.[53]

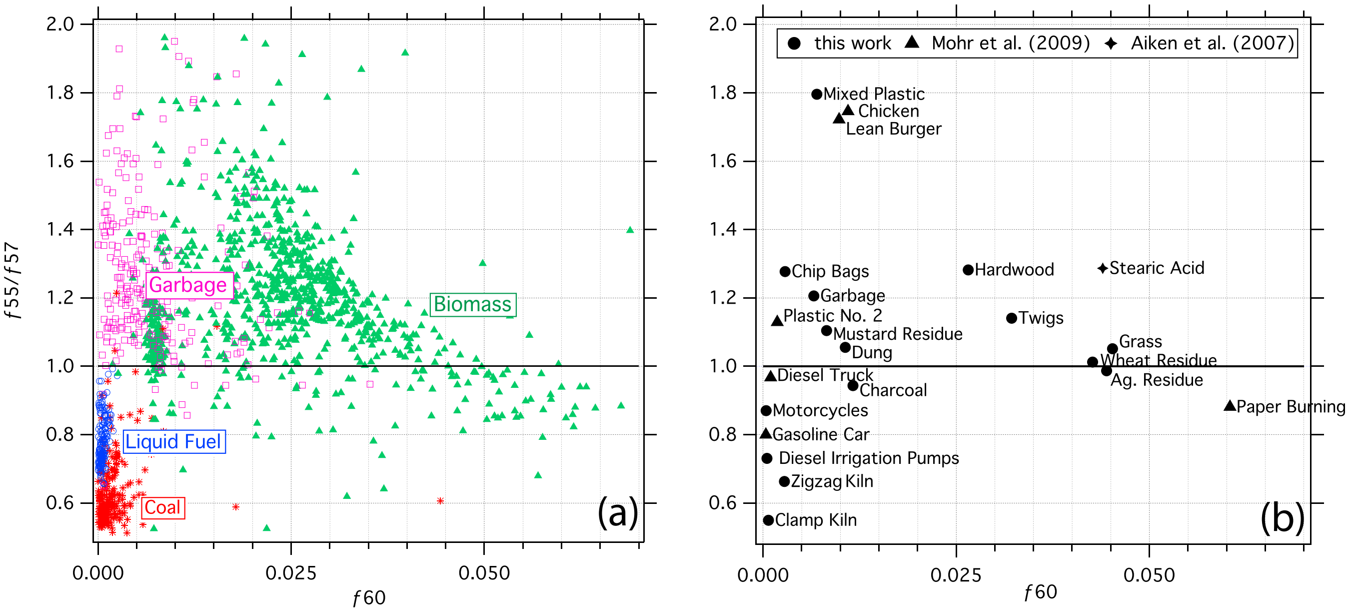

Figure 4. Ratio of f_{55} to f_{57} versus f_{60} for 0.1 Hz source sampling profiles (panel A) and the average from each source type (panel B). Panel A profiles from the sampled sources are grouped by fuel type. Biomass (green triangles) includes field-tested cooking stoves and agricultural residue burning. Garbage (pink squares) includes mixed refuse and plastic burning. Liquid fuel (blue circles) includes motorcycle and irrigation pump profiles. Coal (red asterisks) includes the two sampled brick kilns. Panel B includes averages from this work and from UMR mass spectral profiles retrieved from Mohr et al.

Emissions from the more efficient coal-fired zigzag brick kiln were observed to have inorganic profiles most similar to the clamp kiln emissions. Large inorganic fractions were observed in the NR-PM_1 mass spectra with sulfate contributing to the majority of mass at 57% of the total (Figure 1o). Other inorganic components contributed significantly less mass with ammonium at 24%, and nitrate and chloride contributing to <1% of the total. The fraction of ammonium for this kiln indicated that sulfate associated with zigzag kiln emissions was only about 30% neutralized. Similar results were observed by Jayarathne et al.[27] and suggested that the majority of the emitted sulfate was in the form of nonneutralized sulfuric acid and ammonium bisulfate. The larger fraction of sulfate detected from the zigzag kiln compared to the clamp kiln was possibly due to the sulfur content of the fuel as elemental analysis of both coals conducted by Stockwell et al.[27] showed that the zigzag kiln coal contained 1.28% sulfur by weight about twice as much sulfur compared to the coal used in the clamp kiln. Further investigation of brick kilns is needed to assess the impact of the coal quality and fuel type on aerosol emissions. Additionally, based on the substantial fraction of inorganic aerosol emissions from the brick kilns, large inorganic mass loadings, in particular sulfate, found in ambient datasets with nearby brick kilns should be considered as markers for coal-fired brickmaking.

Based on the mass spectral data, the organic aerosol emissions from the zigzag brick kiln were some of the most unique of the investigated emission sources in NAMaSTE because of large fractions of nitrogen-containing organic compounds. Dominant organic peaks included m/z 30, m/z 42, m/z 44, m/z 45, m/z 58, and m/z 86 (Figure 1o). High-resolution peak fitting estimates indicate that the peaks are associated with the ion series $C_mH_{2m}N^+$ and $C_mH_{2m+2}N^+$. Figure 3 gives the chopper open, chopper closed (background signal), and difference signal (used to calculate aerosol mass) peak fitting estimates for some major m/z peaks detected from the zigzag emissions. The peak fits indicate that the majority of difference signal at m/z 30 is due to the organic ion CH_4N^+ and not the NO^+as is commonly observed with the detection of inorganic nitrate. (Figure 3). Following the remaining $C_mH_{2m+2}N^+$ series, the peak fits indicate that the major ions detected at m/z 44 was $C_2H_6N^+$, m/z 58 was $C_3H_8N^+$, and 86 was $C_5H_{12}N^+$ (Figure 3). Nonnitrogen-containing ions were also estimated to make up a fraction of the listed UMR peaks but always at lower values. Some of the nitrogen-containing organic peaks were also observed with charcoal burning but at much lower fractions, and the peaks were attributed to aliphatic primary amides or similar compounds. The mechanism responsible for the formation of amine species or other nitrogen-containing compounds from coal and charcoal burning is unknown. Additionally, why the compounds were observed with the zigzag kiln emissions and not clamp kiln emissions, both of which were from coal combustion, is unknown. One potential explanation is the addition of cofired fuels while sampling took place. For example, bagasse, or sugar cane residue, was known to be used as a starter fuel with the zigzag kiln. Ambient volatile organic compound (VOC) sampling in the Kathmandu Valley[58] and within the Northwest Indo-Gangetic Plain[59] has attributed observations of isocyanic acid, formamide, and acetamide to the photochemical oxidation of alkyl amides and amines emitted from biomass burning. The connection with amides and amines suggest that the cofiring of biomass was the likely source of nitrogen-containing organic peaks from the zigzag kiln and additional evidence can be found in Sarkar et al.[22] who estimated that 6.9% of the ambient formamide and 7.5% of the ambient acetamide observed within the wintertime Kathmandu Valley could be sourced to cofired brick-making kilns. Further characterization of coal-fired and cofired brick kilns is needed to understand if emissions of nitrogen-containing organics are pervasive with brick making emissions the potential role of cofired biomass. If amine and amide aerosol ions are common

https://doi.org/10.1021/acsearthspacechem.2c00173
ACS Earth Space Chem. 2022, 6, 2619−2631

with brick kilns, they could be useful marker ions for coal-fired brick making depending on their atmospheric stability.

3.2. Source Identification with UMR Mapping. The relative ratios between UMR organic ion fractions retrieved from AMS mass spectra are established tools for evaluating the chemical characteristics of ambient aerosol. One example used by the AMS community to identify the photochemical age of ambient aerosol is the ratio of f_{44} to f_{43} or a measure of oxygenation of organic aerosol.[60] Another commonly used tool is the relationship between f_{44} and f_{60} to evaluate the photochemical age of biomass burning aerosol.[45] Here, we propose the use of the ratio of organic ion fraction f_{55} to f_{57} versus f_{60} to plot and identify the emission sources of primary organic ambient aerosol found in South Asia and globally as seen in Figure 4.

One basis for this type of analysis is the concept that f_{60}, a marker for levoglucosan-containing aerosol, is an indicator of biomass burning and therefore a method to differentiate biomass sources from nonbiomass sources. Figure 4a, for example, demonstrates that mass spectral profiles from biomass burning sources in this study, including wood- and dung-fired cooking stoves, and agricultural residue burning yield f_{60} mostly >0.005 with an average value of 0.022. Fossil fuel emission sources including the liquid-fueled sources (i.e., motorcycles and irrigation pumps) and coal-fired brick kilns yielded f_{60} values <0.005 and often with values at or below detection limits for organics at m/z 60 (Figure 4a). The garbage burning emissions were found to have a similar range to the fossil fuel emissions from plastic burning, with some 0.1 Hz profiles yielding f_{60} similar biomass burning sources, likely due to biomass (e.g., paper, cardboard, etc.) contained in the mixed refuse. Thus, using f_{60} to identify biomass versus nonbiomass aerosol emissions from unknown sources with UMR mass spectral profiles is trivial, but tools are needed for further discrimination of nonbiomass sources like garbage burning and liquid fuels.

To better separate and identify nonbiomass source emission types using UMR spectra alone, the ratio between f_{55} and f_{57} (f_{55}:f_{57}) can be used. As discussed with the high-resolution peak fitting estimates in the above sections, the ion series associated with the electron ionization of saturated hydrocarbons (i.e., $C_nH_{2n+1}^+$ and $C_nH_{2n-1}^+$) is the dominant ion series found in nonbiomass burning mass spectra contributing in sum to greater than 50% of the organic mass, with the exception of the zigzag brick kiln where nitrogen-containing organics were prevalent (Figure 1). The ions from these two saturated hydrocarbon series with the largest overall fraction were always $C_4H_7^+$, found at m/z 55, and $C_4H_9^+$, found at m/z 57, and because of their high signal-to-noise, the ions are ideal candidates to represent the discussed ion series. Based on the observations from this study, it is clear that, of the nonbiomass emission sources, garbage burning was found to have a larger fraction of $C_4H_7^+$ compared to $C_4H_9^+$ and the opposite was found for the liquid and other solid fossil fuel emissions (i.e., brick kilns, motorcycles, irrigation pumps). As seen in Figure 4a, f_{55}:f_{57} for coal burning generally ranged from 0.5 to 0.8 and for liquid fuel burning ranged from 0.7 to 0.9. Alternatively, garbage burning emissions were found to have f_{55}:f_{57} > 1.0 and ranged to 2.0 (Figure 4a). These relative values demonstrate that fresh emissions from the studied nonbiomass fuel sources can be broadly differentiated with f_{55}:f_{57}. The fraction ratio has been used in a similar application by Robinson et al.,[61] who used f_{55}:f_{57} > 1.6 to identify cooking-like organic aerosol emissions in ambient mobile sampling conducted in the United States.

f_{55}:f_{57} and f_{60} from the average mass spectra for the tested emission sources can be found in Figure 4b. The figure highlights trends already uncovered with the fuel-based analysis, but also shows the relative variability between emission sources of a similar fuel type. Among the garbage burning samples, mixed plastic burning was found to have the largest f_{55}:f_{57} at 1.8 followed by chip bag burning (f_{55}:f_{57} = 1.27) and mixed garbage burning (f_{55}:f_{57} = 1.21). The range in garbage burning is likely due to compositional differences in the refuse, for example, the percentage of polyvinyl chloride, polystyrene, or polyethylene plastics, or the relative amount of nonplastics, may play a role. The location of the open garbage emissions in f_{55}:f_{57} vs f_{60} space is consistent with average mass spectra from lab-based high-density polyethylene (HDPE), or plastic number 2, burning emissions from Mohr et al.[41] (Figure 4b). Looking at the fossil fuel emission sources, the coal-fired brick kilns were found to have the lowest average f_{55}:f_{57} with values <0.65, followed by the diesel-fueled irrigation pumps (f_{55}:f_{57} = 0.73), then finally with motorcycle emission with a f_{55}:f_{57} of 0.87. Vehicle emission mass spectra from Mohr et al.[41] show that gasoline-powered cars and diesel-powered trucks have similar f_{55}:f_{57} vs f_{60} compared to the liquid-fueled emission sources in this study (Figure 4b). However, the position is reversed compared to our study, pointing to combustion efficiency, variability in fuel composition, or percentage of uncombusted fuel in the exhaust as possible factors in f_{55}:f_{57} values for any given fuel type. Some evidence for the influence of uncombusted fuel in f_{55}:f_{57} values comes from Canagaratna et al.[56] who found f_{55}:f_{57} close to 1 from diesel bus emission mass spectra and decreasing values from uncombusted aerosolized lubricating oil and diesel fuel.

Turning to the biomass burning emission sources, the sources have an average f_{60} greater than 0.008, but with the largest f_{60} generally observed with agricultural residue burning ($f60 \approx 0.045$) and followed by wood-fueled cookstoves ($f_{60} \approx$ 0.030). These values are consistent with average paper burning mass spectra retrieved from Mohr et al.,[41] which gives an f_{60} value of 0.060, and should produce the most levoglucosan of any source since paper is primarily composed of cellulose. The lowest f_{60} among the biomass sources was observed with dung burning, charcoal biobriquette burning, and mustard residue burning ($f_{60} \approx 0.010$) (Figure 4b). The low f_{60} from mustard residue burning was unexpected as it is an outlier from the other crop burning samples. However, the mustard residue was the only agricultural residue burning in NAMaSTE to exhibit levels of gas-phase glycolaldehyde, a product of cellulose pyrolysis, below detection limits.[27] The low f_{60} and gas-phase glycolaldehyde observed with mustard residue burning suggests the crop fuel was low in cellulose or was mixed with nonbiomass fuel. Similarly, the lower f_{60} observed with charcoal and dung burning is likely explained by the low cellulose content in those fuels compared to wood and paper burning.

Although the f_{55}:f_{57} vs f_{60} plotting presented in this study provides a framework for identifying unknown emission sources in ambient datasets, there are some limitations. This study was not an exhaustive investigation of all organic aerosol sources in South Asia, and the mass spectra from other industrial, commercial, or domestic activities in South Asia are not known. One source that was not sampled in this study, but included in Figure 4b, is meat cooking. Meat cooking

https://doi.org/10.1021/acsearthspacechem.2c00173
ACS Earth Space Chem. 2022, 6, 2619−2631

emissions are known to be responsible for large f_{55} values, and organics at m/z 55 have previously been used as a molecular marker for these emissions with ambient measurements in Barcelona.[62] In Figure 4b, the average mass spectra from lab-based chicken and lean burger cooking fall into a similar space (f_{55}:f_{57} = 1.7; f_{60} = 0.01) as the plastic burning average. The intersection of meat cooking and garbage burning emissions in f_{55}:f_{57} vs f_{60} space could cause misidentification of aerosol emission sources in some ambient datasets; however, meat cooking emissions are expected to be minor compared to garbage burning emission in South Asia and other developing regions of the world due to diets and the pervasiveness of garbage burning.[50] Additionally, to prevent the confounding of these emission sources, it is recommended that previously discussed markers are used to corroborate any ambient mass spectra as garbage burning. For example, enhanced organic aerosol signal at m/z 104 or m/z 166 would be useful identifiers. The presence of enhanced chloride in UMR AMS mass spectra and HCl in high-resolution mass spectra would further validate the suspected identification of garbage burning emissions. If offline filter-based aerosol sampling is available, the garbage burning tracers TPB and Sb could be used. Finally, there is no perfect tool for the identification of aerosol emission sources with UMR mass spectra alone. The proposed UMR mapping, however, is a convenient tool with the potential to broadly categorize the mass spectra of ambient air retrieved with UMR aerosol mass spectrometers.

4. CONCLUSIONS

Mini AMS aerosol mass spectra were retrieved from the emissions of combustion sources common to South Asia. Historically, the chemical makeup of these submicron aerosol emissions are not well characterized because of limited field measurements, and because many of the investigated sources have not previously been studied with online aerosol mass spectrometry. Here, we present the nonrefractory UMR profiles, which can be used as a basis for future AMS ambient or emission measurements in South Asia and throughout the developing world where activities like garbage burning, brick making, or dung-fueled cooking are prevalent, to name a few. For example, the UMR profiles give new evidence of tracer ions for garbage burning associated with plastics combustion that may be useful in ambient source apportionment. Profiles from other sources like the wood burning cookstoves and agricultural residue burning show commonality to previous lab and field-based measurements of biomass burning demonstrating that biomass source profiles from outside of South Asia may be useful in understanding South Asian air quality. The proposed UMR organic ion mapping using f_{55}, f_{57}, and f_{60} gives additional basis for characterizing the contribution of various emission types to ambient aerosol datasets retrieved with aerosol mass spectrometers and could be complimentary to source identification by positive matrix factorization or other source apportionment tools. High-resolution treatment of the UMR profiles from the investigated sources provides a foundation for similar signal processing when high-resolution mass spectral measurements are not available. Evidence of significant fractions of nitrogen-containing organic aerosol from the high-resolution fits of profiles from the charcoal-fueled cookstove and one of the coal-fired brick kilns is noteworthy because of the uncertain influence of these species in the ambient environment. However, it is uncertain if these organic compounds are ubiquitous with charcoal burning and brick making or what processes control their emissions. The evidence of nitrogen-containing organics, therefore, provides motivation for additional measurements of these emission sources.

■ ASSOCIATED CONTENT

Supporting Information

The Supporting Information is available free of charge at https://pubs.acs.org/doi/10.1021/acsearthspacechem.2c00173.

Table of sampled emission sources (Supplementary Material-1), figure of organic aerosol only mass spectra for the field-tested cookstove emissions (Supplementary Material-2), average mass spectra for lab and field-tested wood burning cookstove emissions (Supplementary Material-3), average mass spectra for lab and field-tested dung burning cookstove emissions (Supplementary Material-4), figure of organic only mass spectra for the field-tested agricultural residue burning emissions (Supplementary Material-5), figure of organic only mass spectra for the field-tested garbage burning emissions (Supplementary Material-6), figure of organic only mass spectra for the brick kiln emissions (Supplementary Material-7), figure of organic only mass spectra for the charcoal burning emissions (Supplementary Material-8), figure of organic only mass spectra from m/z 120 to m/z 160 from charcoal burning emissions (Supplementary Material-9) and figure of organic only mass spectra for the sampled engine exhaust emission (Supplementary Material-10) (PDF)

■ AUTHOR INFORMATION

Corresponding Authors

J. Douglas Goetz − *Laboratory for Atmospheric and Space Physics, University of Colorado at Boulder, Boulder, Colorado 80303, United States;* orcid.org/0000-0003-0824-1215; Email: doug.goetz@lasp.colorado.edu

Peter F. DeCarlo − *Department of Environmental Health and Engineering, Johns Hopkins University, Baltimore, Maryland 21205, United States;* orcid.org/0000-0001-6385-7149; Email: pdecarl1@jhu.edu

Authors

Michael R. Giordano − *Department of Civil, Architectural, and Environmental Engineering, Drexel University, Philadelphia, Pennsylvania 19104, United States;* Present Address: Carnegie Mellon University, Center for Atmospheric Particle Studies, Pittsburgh, Pennsylvania 15213, United States (M.R.G.)

Chelsea E. Stockwell − *Department of Chemistry, University of Montana, Missoula, Montana 59812, United States;* Present Address: Cooperative Institute for Research in Environmental Sciences, University of Colorado, Boulder, Colorado 80309, United States (C.E.S.).; orcid.org/0000-0003-3462-2126

Prakash V. Bhave − *International Centre for Integrated Mountain Development (ICIMOD), Lalitpur 44700, Nepal;* Present Address: Agricultural Institute, North Carolina State University, Raleigh, North Carolina 27607, United States (P.V.B.).

https://doi.org/10.1021/acsearthspacechem.2c00173
ACS Earth Space Chem. 2022, 6, 2619−2631

Praveen S. Puppala – *International Centre for Integrated Mountain Development (ICIMOD), Lalitpur 44700, Nepal*
Arnico K. Panday – *International Centre for Integrated Mountain Development (ICIMOD), Lalitpur 44700, Nepal;* Present Address: Ullens Education Foundation, Khumaltar, Lalitpur 44700, Nepal (A.K.P.).
Thilina Jayarathne – *Department of Chemistry, University of Iowa, Iowa City, Iowa 52242, United States*
Elizabeth A. Stone – *Department of Chemistry and Department of Chemical and Biochemical Engineering, University of Iowa, Iowa City, Iowa 52242, United States;* orcid.org/0000-0003-0078-141X
Robert J. Yokelson – *Department of Chemistry, University of Montana, Missoula, Montana 59812, United States*

Complete contact information is available at:
https://pubs.acs.org/10.1021/acsearthspacechem.2c00173

Author Contributions

The manuscript was written through contributions of all authors. All authors have given approval to the final version of the manuscript.

Funding

J.D.G., M.R.G., and P.F.D. were funded by the National Science Foundation AGS award 1461458. T.J. and E.A.S. were funded by the National Science Foundation AGS award 1351616. C.E.S. and R.J.Y. were funded by the National Science Foundation AGS award 1349976 and, R.J.Y. was additionally supported by the NASA Earth Science Division award NNX14AP45G. ICIMOD participant including P.V.B., P.S.P., and A.K.P. were supported by ICIMOD, which is contributed to by the governments of Afghanistan, Australia, Austria, Bangladesh, Bhutan, China, India, Myanmar, Nepal, Norway, Pakistan, Switzerland, and the United Kingdom.

Notes

The authors declare no competing financial interest.

■ ACKNOWLEDGMENTS

The authors would like to thank the logistics and support team in Nepal, which included numerous personnel from ICIMOD, MinErgy Pvt. Ltd., and RETS. We would like to acknowledge the proficiency and expertise of Sanubabu B. Dangol and the MinErgy team, who were integral to finding and gaining access to field sites for this study. A special thanks to Karma Sherpa and Nawraj, who were both central parts of the field team, and without whom, this work would not be possible and possibly less enjoyable. We would also like to acknowledge the assistance of Wolfgang Nadler of Drexel University for his assistance in the field measurements. We thank the villagers of Nawalparasi for their generosity and hospitality.

■ REFERENCES

(1) Chen, B. H.; Hong, C. J.; Pandey, M. R.; Smith, K. R. Indoor Air Pollution in Developing Countries. *World Health Stat. Q.* **1990**, *43*, 127–138.

(2) Guttikunda, S. K.; Goel, R.; Pant, P. Nature of Air Pollution, Emission Sources, and Management in the Indian Cities. *Atmos. Environ.* **2014**, *95*, 501–510.

(3) Lelieveld, J.; Crutzen, P. J.; Ramanathan, V.; Andreae, M. O.; Brenninkmeijer, C. A. M.; Campos, T.; Cass, G. R.; Dickerson, R. R.; Fischer, H.; de Gouw, J. A.; Hansel, A.; Jefferson, A.; Kley, D.; de Laat, A. T. J.; Lal, S.; Lawrence, M. G.; Lobert, J. M.; Mayol-Bracero, O. L.; Mitra, A. P.; Novakov, T.; Oltmans, S. J.; Prather, K. A.; Reiner, T.; Rodhe, H.; Scheeren, H. A.; Sikka, D.; Williams, J. The Indian Ocean Experiment: Widespread Air Pollution from South and Southeast Asia. *Science* **2001**, *291*, 1031–1036.

(4) Ohara, T.; Akimoto, H.; Kurokawa, J.; Horii, N.; Yamaji, K.; Yan, X.; Hayasaka, T. An Asian Emission Inventory of Anthropogenic Emission Sources for the Period 1980–2020. *Atmos. Chem. Phys.* **2007**, *7*, 4419–4444.

(5) Panday, A. K.; Prinn, R. G. Diurnal Cycle of Air Pollution in the Kathmandu Valley, Nepal: Observations. *J. Geophys. Res.: Atmos.* **2009**, *114* (), DOI: 10.1029/2008JD009777.

(6) Lawrence, M. G.; Lelieveld, J. Atmospheric Pollutant Outflow from Southern Asia: A Review. *Atmos. Chem. Phys.* **2010**, *10*, 11017–11096.

(7) Yu, P.; Rosenlof, K. H.; Liu, S.; Telg, H.; Thornberry, T. D.; Rollins, A. W.; Portmann, R. W.; Bai, Z.; Ray, E. A.; Duan, Y.; Pan, L. L.; Toon, O. B.; Bian, J.; Gao, R.-S. Efficient Transport of Tropospheric Aerosol into the Stratosphere via the Asian Summer Monsoon Anticyclone. *Proc. Natl. Acad. Sci. U. S. A.* **2017**, *114*, 6972–6977.

(8) Pandey, A.; Sadavarte, P.; Rao, A.; Venkataraman, C. Trends in Multi-Pollutant Emissions from a Technology-Linked Inventory for India: II. Residential, Agricultural and Informal Industry Sectors. *Atmos. Environ.* **2014**, *99*, 341–352.

(9) Reddy, M. S.; Venkataraman, C. Inventory of Aerosol and Sulphur Dioxide Emissions from India: I—Fossil Fuel Combustion. *Atmos. Environ.* **2002**, *36*, 677–697.

(10) Weyant, C.; Athalye, V.; Ragavan, S.; Rajarathnam, U.; Lalchandani, D.; Maithel, S.; Baum, E.; Bond, T. C. Emissions from South Asian Brick Production. *Environ. Sci. Technol.* **2014**, *48*, 6477–6483.

(11) Venkataraman, C.; Habib, G.; Eiguren-Fernandez, A.; Miguel, A. H.; Friedlander, S. K. Residential Biofuels in South Asia: Carbonaceous Aerosol Emissions and Climate Impacts. *Science* **2005**, *307*, 1454–1456.

(12) World Health Organization *Fuel For Life: Houshold Energy and Health*; World Health Organization, 2006, http://www.who.int/indoorair/publications/fuelforlife/en/.

(13) Lim, S. S.; Vos, T.; Flaxman, A. D.; Danaei, G.; Shibuya, K.; Adair-Rohani, H.; Amann, M.; Anderson, H. R.; Andrews, K. G.; Aryee, M.; Atkinson, C.; Bacchus, L. J.; Bahalim, A. N.; Balakrishnan, K.; Balmes, J.; Barker-Collo, S.; Baxter, A.; Bell, M. L.; Blore, J. D.; Blyth, F.; Bonner, C.; Borges, G.; Bourne, R.; Boussinesq, M.; Brauer, M.; Brooks, P.; Bruce, N. G.; Brunekreef, B.; Bryan-Hancock, C.; Bucello, C.; Buchbinder, R.; Bull, F.; Burnett, R. T.; Byers, T. E.; Calabria, B.; Carapetis, J.; Carnahan, E.; Chafe, Z.; Charlson, F.; Chen, H.; Chen, J. S.; Cheng, A. T.; Child, J. C.; Cohen, A.; Colson, K. E.; Cowie, B. C.; Darby, S.; Darling, S.; Davis, A.; Degenhardt, L.; Dentener, F.; Des Jarlais, D. C.; Devries, K.; Dherani, M.; Ding, E. L.; Dorsey, E. R.; Driscoll, T.; Edmond, K.; Ali, S. E.; Engell, R. E.; Erwin, P. J.; Fahimi, S.; Falder, G.; Farzadfar, F.; Ferrari, A.; Finucane, M. M.; Flaxman, S.; Fowkes, F. G.; Freedman, G.; Freeman, M. K.; Gakidou, E.; Ghosh, S.; Giovannucci, E.; Gmel, G.; Graham, K.; Grainger, R.; Grant, B.; Gunnell, D.; Gutierrez, H. R.; Hall, W.; Hoek, H. W.; Hogan, A.; Hosgood, H. D., 3rd; Hoy, D.; Hu, H.; Hubbell, B. J.; Hutchings, S. J.; Ibeanusi, S. E.; Jacklyn, G. L.; Jasrasaria, R.; Jonas, J. B.; Kan, H.; Kanis, J. A.; Kassebaum, N.; Kawakami, N.; Khang, Y. H.; Khatibzadeh, S.; Khoo, J. P.; Kok, C.; Laden, F.; Lalloo, R.; Lan, Q.; Lathlean, T.; Leasher, J. L.; Leigh, J.; Li, Y.; Lin, J. K.; Lipshultz, S. E.; London, S.; Lozano, R.; Lu, Y.; Mak, J.; Malekzadeh, R.; Mallinger, L.; Marcenes, W.; March, L.; Marks, R.; Martin, R.; McGale, P.; McGrath, J.; Mehta, S.; Mensah, G. A.; Merriman, T. R.; Micha, R.; Michaud, C.; Mishra, V.; Mohd Hanafiah, K.; Mokdad, A. A.; Morawska, L.; Mozaffarian, D.; Murphy, T.; Naghavi, M.; Neal, B.; Nelson, P. K.; Nolla, J. M.; Norman, R.; Olives, C.; Omer, S. B.; Orchard, J.; Osborne, R.; Ostro, B.; Page, A.; Pandey, K. D.; Parry, C. D.; Passmore, E.; Patra, J.; Pearce, N.; Pelizzari, P. M.; Petzold, M.; Phillips, M. R.; Pope, D.; Pope, C. A., 3rd; Powles, J.; Rao, M.; Razavi, H.; Rehfuess, E. A.; Rehm, J. T.; Ritz, B.; Rivara, F. P.; Roberts, T.; Robinson, C.; Rodriguez-Portales, J. A.; Romieu, I.; Room, R.; Rosenfeld, L. C.; Roy, A.; Rushton, L.; Salomon, J. A.; Sampson, U.;

Sanchez-Riera, L.; Sanman, E.; Sapkota, A.; Seedat, S.; Shi, P.; Shield, K.; Shivakoti, R.; Singh, G. M.; Sleet, D. A.; Smith, E.; Smith, K. R.; Stapelberg, N. J.; Steenland, K.; Stockl, H.; Stovner, L. J.; Straif, K.; Straney, L.; Thurston, G. D.; Tran, J. H.; Van Dingenen, R.; van Donkelaar, A.; Veerman, J. L.; Vijayakumar, L.; Weintraub, R.; Weissman, M.; White, R. A.; Whiteford, H.; Wiersma, S. T.; Wilkinson, J. D.; Williams, H. C.; Williams, W.; Wilson, N.; Woolf, A. D.; Yip, P.; Zielinski, J. M.; Lopez, A. D.; Murray, C. J.; Ezzati, M.; AlMazroa, M. A.; Memish, Z. A. A Comparative Risk Assessment of Burden of Disease and Injury Attributable to 67 Risk Factors and Risk Factor Clusters in 21 Regions, 1990-2010: A Systematic Analysis for the Global Burden of Disease Study 2010. *Lancet* **2012**, *380*, 2224−2260.

(14) Streets, D. G.; Bond, T. C.; Carmichael, G. R.; Fernandes, S. D.; Fu, Q.; He, D.; Klimont, Z.; Nelson, S. M.; Tsai, N. Y.; Wang, M. Q.; Woo, J. H.; Yarber, K. F. An Inventory of Gaseous and Primary Aerosol Emissions in Asia in the Year 2000. *J. Geophys. Res.: Atmos.* **2003**, *108* (), DOI: 10.1029/2002JD003093.

(15) Hakkim, H.; Kumar, A.; Annadate, S.; Sinha, B.; Sinha, V. RTEII: A New High-Resolution (0.1° × 0.1°) Road Transport Emission Inventory for India of 74 Speciated NMVOCs, CO, NOx, NH3, CH4, CO2, PM2.5 Reveals Massive Overestimation of NOx and CO and Missing Nitromethane Emissions by Existing Inventories. *Atmos. Environ.: X* **2021**, *11*, 100118.

(16) Kumar, R.; Barth, M. C.; Nair, V. S.; Pfister, G. G.; Suresh Babu, S.; Satheesh, S. K.; Krishna Moorthy, K.; Carmichael, G. R.; Lu, Z.; Streets, D. G. Sources of Black Carbon Aerosols in South Asia and Surrounding Regions during the Integrated Campaign for Aerosols, Gases and Radiation Budget (ICARB). *Atmos. Chem. Phys.* **2015**, *15*, 5415−5428.

(17) Kurokawa, J.; Ohara, T.; Morikawa, T.; Hanayama, S.; Janssens-Maenhout, G.; Fukui, T.; Kawashima, K.; Akimoto, H. Emissions of Air Pollutants and Greenhouse Gases over Asian Regions during 2000−2008: Regional Emission Inventory in ASia (REAS) Version 2. *Atmos. Chem. Phys.* **2013**, *13*, 11019−11058.

(18) Gustafsson, Ö.; Kruså, M.; Zencak, Z.; Sheesley, R. J.; Granat, L.; Engström, E.; Praveen, P. S.; Rao, P. S. P.; Leck, C.; Rodhe, H. Brown Clouds over South Asia: Biomass or Fossil Fuel Combustion? *Science* **2009**, *323*, 495−498.

(19) Chowdhury, Z.; Zheng, M.; Schauer, J. J.; Sheesley, R. J.; Salmon, L. G.; Cass, G. R.; Russell, A. G. Speciation of Ambient Fine Organic Carbon Particles and Source Apportionment of PM2.5 in Indian Cities. *J. Geophys. Res.: Atmos.* **2007**, *112* (), DOI: 10.1029/2007JD008386.

(20) Stone, E.; Schauer, J.; Quraishi, T. A.; Mahmood, A. Chemical Characterization and Source Apportionment of Fine and Coarse Particulate Matter in Lahore, Pakistan. *Atmos. Environ.* **2010**, *44*, 1062−1070.

(21) Kim, B. M.; Park, J.-S.; Kim, S.-W.; Kim, H.; Jeon, H.; Cho, C.; Kim, J.-H.; Hong, S.; Rupakheti, M.; Panday, A. K.; Park, R. J.; Hong, J.; Yoon, S.-C. Source Apportionment of PM10 Mass and Particulate Carbon in the Kathmandu Valley. *Nepal Atmos. Environ.* **2015**, *123*, 190−199.

(22) Sarkar, C.; Sinha, V.; Sinha, B.; Panday, A. K.; Rupakheti, M.; Lawrence, M. G. Source Apportionment of NMVOCs in the Kathmandu Valley during the SusKat-ABC International Field Campaign Using Positive Matrix Factorization. *Atmos. Chem. Phys.* **2017**, *17*, 8129−8156.

(23) Islam, M. R.; Jayarathne, T.; Simpson, I. J.; Werden, B.; Maben, J.; Gilbert, A.; Praveen, P. S.; Adhikari, S.; Panday, A. K.; Rupakheti, M.; Blake, D. R.; Yokelson, R. J.; DeCarlo, P. F.; Keene, W. C.; Stone, E. A. Ambient Air Quality in the Kathmandu Valley, Nepal, during the Pre-Monsoon: Concentrations and Sources of Particulate Matter and Trace Gases. *Atmos. Chem. Phys.* **2020**, *20*, 2927−2951.

(24) Islam, M.; Li, T.; Mahata, K.; Khanal, N.; Werden, B.; Giordano, M. R.; Praveen, P. S.; Dhital, N. B.; Gurung, A.; Panday, A. K.; Joshi, I. B.; Poudel, S. P.; Wang, Y.; Saikawa, E.; Yokelson, R. J.; DeCarlo, P. F.; Stone, E. A. Wintertime Air Quality in Lumbini, Nepal: Sources of Fine Particle Organic Carbon. *ACS Earth Space Chem.* **2021**, *5*, 226−238.

(25) Saikawa, E.; Wu, Q.; Zhong, M.; Avramov, A.; Ram, K.; Stone, E. A.; Stockwell, C. E.; Jayarathne, T.; Panday, A. K.; Yokelson, R. J. Garbage Burning in South Asia: How Important Is It to Regional Air Quality? *Environ. Sci. Technol.* **2020**, *54*, 9928−9938.

(26) Tobler, A.; Bhattu, D.; Canonaco, F.; Lalchandani, V.; Shukla, A.; Thamban, N. M.; Mishra, S.; Srivastava, A. K.; Bisht, D. S.; Tiwari, S.; Singh, S.; Močnik, G.; Baltensperger, U.; Tripathi, S. N.; Slowik, J. G.; Prévôt, A. S. H. Chemical Characterization of PM2.5 and Source Apportionment of Organic Aerosol in New Delhi, India. *Sci. Total Environ.* **2020**, *745*, 140924.

(27) Stockwell, C. E.; Christian, T. J.; Goetz, J. D.; Jayarathne, T.; Bhave, P. V.; Praveen, P. S.; Adhikari, S.; Maharjan, R.; DeCarlo, P. F.; Stone, E. A.; Saikawa, E.; Blake, D. R.; Simpson, I. J.; Yokelson, R. J.; Panday, A. K. Nepal Ambient Monitoring and Source Testing Experiment (NAMaSTE): Emissions of Trace Gases and Light-Absorbing Carbon from Wood and Dung Cooking Fires, Garbage and Crop Residue Burning, Brick Kilns, and Other Sources. *Atmos. Chem. Phys.* **2016**, *16*, 11043−11081.

(28) Goetz, J. D.; Giordano, M. R.; Stockwell, C. E.; Christian, T. J.; Maharjan, R.; Adhikari, S.; Bhave, P. V.; Praveen, P. S.; Panday, A. K.; Jayarathne, T.; Stone, E. A.; Yokelson, R. J.; DeCarlo, P. F. Speciated Online PM1 from South Asian Combustion Sources − Part 1: Fuel-Based Emission Factors and Size Distributions. *Atmos. Chem. Phys.* **2018**, *18*, 14653−14679.

(29) Jayarathne, T.; Stockwell, C. E.; Bhave, P. V.; Praveen, P. S.; Rathnayake, C. M.; Islam, M. R.; Panday, A. K.; Adhikari, S.; Maharjan, R.; Goetz, J. D.; DeCarlo, P. F.; Saikawa, E.; Yokelson, R. J.; Stone, E. A. Nepal Ambient Monitoring and Source Testing Experiment (NAMaSTE): Emissions of Particulate Matter from Wood- and Dung-Fueled Cooking Fires, Garbage and Crop Residue Burning, Brick Kilns, and Other Sources. *Atmos. Chem. Phys.* **2018**, *18*, 2259−2286.

(30) Werden, B.; Giordano, M. R.; Goetz, J. D.; Islam, M. R.; Bhave, P. V.; Praveen, P. S.; Rupakheti, M.; Saikawa, E.; Panday, A. K.; Yokelson, R. J.; Stone, E. A.; DeCarlo, P. F. Pre-Monsoon Submicron Aerosol Composition and Source Contribution in the Kathmandu Valley, Nepal. *Environ. Sci.: Atmos.* **2022**, *2*, 978−999.

(31) Manadhar, U. M.; Dangol, S. B. Study on Evaluating Energy Conservation Potential of Bricks Production in SAARC Countries: A Report for Nepal. *SAARC Energy Centre* **2013**.

(32) Drewnick, F.; Hings, S. S.; DeCarlo, P.; Jayne, J. T.; Gonin, M.; Fuhrer, K.; Weimer, S.; Jimenez, J. L.; Demerjian, K. L.; Borrmann, S.; Worsnop, D. R. A New Time-of-Flight Aerosol Mass Spectrometer (TOF-AMS)—Instrument Description and First Field Deployment. *Aerosol Sci. Technol.* **2005**, *39*, 637−658.

(33) Fröhlich, R.; Cubison, M. J.; Slowik, J. G.; Bukowiecki, N.; Prévôt, A. S. H.; Baltensperger, U.; Schneider, J.; Kimmel, J. R.; Gonin, M.; Rohner, U.; Worsnop, D. R.; Jayne, J. T. The ToF-ACSM: A Portable Aerosol Chemical Speciation Monitor with TOFMS Detection. *Atmos. Meas. Technol.* **2013**, *6*, 3225−3241.

(34) Allan, J. D.; Delia, A. E.; Coe, H.; Bower, K. N.; Alfarra, M. R.; Jimenez, J. L.; Middlebrook, A. M.; Drewnick, F.; Onasch, T. B.; Canagaratna, M. R.; Jayne, J. T.; Worsnop, D. R. A Generalised Method for the Extraction of Chemically Resolved Mass Spectra from Aerodyne Aerosol Mass Spectrometer Data. *J. Aerosol Sci.* **2004**, *35*, 909−922 http://dx.doi.org/10.1016/j.jaerosci.2004.02.007.

(35) Collier, S.; Zhang, Q. Gas-Phase CO2 Subtraction for Improved Measurements of the Organic Aerosol Mass Concentration and Oxidation Degree by an Aerosol Mass Spectrometer. *Environ. Sci. Technol.* **2013**, *47*, 14324−14331.

(36) Alfarra, M. R.; Prevot, A. S. H.; Szidat, S.; Sandradewi, J.; Weimer, S.; Lanz, V. A.; Schreiber, D.; Mohr, M.; Baltensperger, U. Identification of the Mass Spectral Signature of Organic Aerosols from Wood Burning Emissions. *Environ. Sci. Technol.* **2007**, *41*, 5770−5777.

(37) Ng, N. L.; Canagaratna, M. R.; Jimenez, J. L.; Zhang, Q.; Ulbrich, I. M.; Worsnop, D. R. Real-Time Methods for Estimating

Organic Component Mass Concentrations from Aerosol Mass Spectrometer Data. *Environ. Sci. Technol.* **2011**, *45*, 910−916.

(38) Schneider, J.; Weimer, S.; Drewnick, F.; Borrmann, S.; Helas, G.; Gwaze, P.; Schmid, O.; Andreae, M. O.; Kirchner, U. Mass Spectrometric Analysis and Aerodynamic Properties of Various Types of Combustion-Related Aerosol Particles. *Int. J. Mass Spectrom.* **2006**, *258*, 37−49.

(39) Simoneit, B. R. T.; Schauer, J. J.; Nolte, C. G.; Oros, D. R.; Elias, V. O.; Fraser, M. P.; Rogge, W. F.; Cass, G. R. Levoglucosan, a Tracer for Cellulose in Biomass Burning and Atmospheric Particles. *Atmos. Environ.* **1999**, *33*, 173−182.

(40) Christian, T. J.; Yokelson, R. J.; Cárdenas, B.; Molina, L. T.; Engling, G.; Hsu, S. C. Trace Gas and Particle Emissions from Domestic and Industrial Biofuel Use and Garbage Burning in Central Mexico. *Atmos. Chem. Phys.* **2010**, *10*, 565−584.

(41) Mohr, C.; Huffman, J. A.; Cubison, M. J.; Aiken, A. C.; Docherty, K. S.; Kimmel, J. R.; Ulbrich, I. M.; Hannigan, M.; Jimenez, J. L. Characterization of Primary Organic Aerosol Emissions from Meat Cooking, Trash Burning, and Motor Vehicles with High-Resolution Aerosol Mass Spectrometry and Comparison with Ambient and Chamber Observations. *Environ. Sci. Technol.* **2009**, *43*, 2443−2449.

(42) Ulbrich, I. M.; Canagaratna, M. R.; Zhang, Q.; Worsnop, D. R.; Jimenez, J. L. Interpretation of Organic Components from Positive Matrix Factorization of Aerosol Mass Spectrometric Data. *Atmos. Chem. Phys.* **2009**, *9*, 2891−2918.

(43) Ulbrich, I. M.; Lechner, M. J.; Jimenez, J. L. *AMS Spectral Database*; University of Minnesota, 2017.

(44) Dzepina, K.; Arey, J.; Marr, L. C.; Worsnop, D. R.; Salcedo, D.; Zhang, Q.; Onasch, T. B.; Molina, L. T.; Molina, M. J.; Jimenez, J. L. Detection of Particle-Phase Polycyclic Aromatic Hydrocarbons in Mexico City Using an Aerosol Mass Spectrometer. *Int. J. Mass Spectrom.* **2007**, *263*, 152−170 http://dx.doi.org/10.1016/j.ijms.2007.01.010.

(45) Cubison, M. J.; Ortega, A. M.; Hayes, P. L.; Farmer, D. K.; Day, D.; Lechner, M. J.; Brune, W. H.; Apel, E.; Diskin, G. S.; Fisher, J. A.; Fuelberg, H. E.; Hecobian, A.; Knapp, D. J.; Mikoviny, T.; Riemer, D.; Sachse, G. W.; Sessions, W.; Weber, R. J.; Weinheimer, A. J.; Wisthaler, A.; Jimenez, J. L. Effects of Aging on Organic Aerosol from Open Biomass Burning Smoke in Aircraft and Laboratory Studies. *Atmos. Chem. Phys.* **2011**, *11*, 12049−12064.

(46) Sheesley, R. J.; Schauer, J. J.; Chowdhury, Z.; Cass, G. R.; Simoneit, B. R. T. Characterization of Organic Aerosols Emitted from the Combustion of Biomass Indigenous to South Asia. *J. Geophys. Res.: Atmos.* **2003**, *108* (), DOI: 10.1029/2002JD002981.

(47) Huffman, J. A.; Docherty, K. S.; Aiken, A. C.; Cubison, M. J.; Ulbrich, I. M.; DeCarlo, P. F.; Sueper, D.; Jayne, J. T.; Worsnop, D. R.; Ziemann, P. J.; Jimenez, J. L. Chemically-Resolved Aerosol Volatility Measurements from Two Megacity Field Studies. *Atmos. Chem. Phys.* **2009**, *9*, 7161−7182.

(48) Zhang, Q.; Jimenez, J. L.; Canagaratna, M. R.; Ulbrich, I. M.; Ng, N. L.; Worsnop, D. R.; Sun, Y. Understanding Atmospheric Organic Aerosols via Factor Analysis of Aerosol Mass Spectrometry: A Review. *Anal. Bioanal. Chem.* **2011**, *401*, 3045−3067.

(49) McLafferty, F. W.; Turecek, A. *Interpretation of Mass Spectra*; University Scientific Books: Mill Valley, CA, 1993.

(50) Wiedinmyer, C.; Yokelson, R. J.; Gullett, B. K. Global Emissions of Trace Gases, Particulate Matter, and Hazardous Air Pollutants from Open Burning of Domestic Waste. *Environ. Sci. Technol.* **2014**, *48*, 9523−9530.

(51) Stein, S.; Mirokhin, D.; Tchekhovskoi, D.; Mallard, G. *The NIST Mass Spectral Search Program for the NIST/EPA/NIH Mass Spectral Library*; The Standard Reference Data Program of NIST, 2001.

(52) Yam, K. L. Cereals, Bakery Products, Snack Foods, and Candy. In *Wiley Encyclopedia of Packaging Technology (3rd Edition)*; John Wiley & Sons, 2009.

(53) Simoneit, B. R. T.; Medeiros, P. M.; Didyk, B. M. Combustion Products of Plastics as Indicators for Refuse Burning in the Atmosphere. *Environ. Sci. Technol.* **2005**, *39*, 6961−6970.

(54) Gadi, R.; Shivani; Sharma, S. K.; Mandal, T. K. Source Apportionment and Health Risk Assessment of Organic Constituents in Fine Ambient Aerosols (PM2.5): A Complete Year Study over National Capital Region of India. *Chemosphere* **2019**, *221*, 583−596.

(55) Haque, M. M.; Kawamura, K.; Deshmukh, D. K.; Fang, C.; Song, W.; Mengying, B.; Zhang, Y.-L. Characterization of Organic Aerosols from a Chinese Megacity during Winter: Predominance of Fossil Fuel Combustion. *Atmos. Chem. Phys.* **2019**, *19*, 5147−5164.

(56) Canagaratna, M. R.; Jayne, J. T.; Ghertner, D. A.; Herndon, S.; Shi, Q.; Jimenez, J. L.; Silva, P. J.; Williams, P.; Lanni, T.; Drewnick, F.; Demerjian, K. L.; Kolb, C. E.; Worsnop, D. R. Chase Studies of Particulate Emissions from In-Use New York City Vehicles. *Aerosol Sci. Technol.* **2004**, *38*, 555−573.

(57) Hu, W. W.; Hu, M.; Yuan, B.; Jimenez, J. L.; Tang, Q.; Peng, J. F.; Hu, W.; Shao, M.; Wang, M.; Zeng, L. M.; Wu, Y. S.; Gong, Z. H.; Huang, X. F.; He, L. Y. Insights on Organic Aerosol Aging and the Influence of Coal Combustion at a Regional Receptor Site of Central Eastern China. *Atmos. Chem. Phys.* **2013**, *13*, 10095−10112.

(58) Sarkar, C.; Sinha, V.; Kumar, V.; Rupakheti, M.; Panday, A.; Mahata, K. S.; Rupakheti, D.; Kathayat, B.; Lawrence, M. G. Overview of VOC Emissions and Chemistry from PTR-TOF-MS Measurements during the SusKat-ABC Campaign: High Acetaldehyde, Isoprene and Isocyanic Acid in Wintertime Air of the Kathmandu Valley. *Atmos. Chem. Phys.* **2016**, *16*, 3979−4003.

(59) Kumar, V.; Chandra, B. P.; Sinha, V. Large Unexplained Suite of Chemically Reactive Compounds Present in Ambient Air Due to Biomass Fires. *Sci. Rep.* **2018**, *8*, 626.

(60) Ng, N. L.; Canagaratna, M. R.; Zhang, Q.; Jimenez, J. L.; Tian, J.; Ulbrich, I. M.; Kroll, J. H.; Docherty, K. S.; Chhabra, P. S.; Bahreini, R.; Murphy, S. M.; Seinfeld, J. H.; Hildebrandt, L.; Donahue, N. M.; DeCarlo, P. F.; Lanz, V. A.; Prévôt, A. S. H.; Dinar, E.; Rudich, Y.; Worsnop, D. R. Organic Aerosol Components Observed in Northern Hemispheric Datasets from Aerosol Mass Spectrometry. *Atmos. Chem. Phys.* **2010**, *10*, 4625−4641.

(61) Robinson, E. S.; Gu, P.; Ye, Q.; Li, H. Z.; Shah, R. U.; Apte, J. S.; Robinson, A. L.; Presto, A. A. Restaurant Impacts on Outdoor Air Quality: Elevated Organic Aerosol Mass from Restaurant Cooking with Neighborhood-Scale Plume Extents. *Environ. Sci. Technol.* **2018**, *52*, 9285−9294.

(62) Mohr, C.; DeCarlo, P. F.; Heringa, M. F.; Chirico, R.; Slowik, J. G.; Richter, R.; Reche, C.; Alastuey, A.; Querol, X.; Seco, R.; Peñuelas, J.; Jiménez, J. L.; Crippa, M.; Zimmermann, R.; Baltensperger, U.; Prévôt, A. S. H. Identification and Quantification of Organic Aerosol from Cooking and Other Sources in Barcelona Using Aerosol Mass Spectrometer Data. *Atmos. Chem. Phys.* **2012**, *12*, 1649−1665.